Basic Research for Acquiring Advanced Pathological Information by Circularly Polarized Light Analysis of Biological Tissue*

Shintaro TODA[*1], Shuhei ICHIKAWA[*2], Tsuyoshi TAKASHIMA[*3] and Eiichi MORII[*3]

[*1] Research Laboratory for Future Technology, Research & Development HQ, ULVAC, Inc., 2-1 Yamadaoka, Suita, Osaka 565-0871, Japan
[*2] Graduate School of Engineering, The University of Osaka, 2-1 Yamadaoka, Suita, Osaka 565-0871, Japan
[*3] Graduate School of Medicine, The University of Osaka, 2-1 Yamadaoka, Suita, Osaka 565-0871, Japan

Non-invasive diagnosis using circularly polarized light (CPL) is a promising next-generation medical technology. In this study, the visible CPL characteristics of human lung adenocarcinoma were evaluated. Cultured cell samples (normal and cancerous) and sliced tissue samples (non-metastatic and metastatic cases) were irradiated with white CPL, and the polarization state of the transmitted light was analyzed by the polarizer rotation method. As a result, the depolarization ratio and its circular dichrosim (CD) were larger in the cancerous cells (or tumor region) than in the normal ones in all samples. In addition, there was a gap between the different CDs of the normal and the tumor region in each non-metastatic and metastatic sliced tissue sample. These findings suggest that polarization parameters may be applicable to distinguishing between normal and cancerous cells (or tumor regions) and to evaluating the malignancy of a cancer.

1. Introduction

1.1 Medical photonics

Malignant neoplasms (cancers) are the most common cause of death in Japan[1]. While the importance of early cancer detection is obvious, there remain social issues such as a shortage of pathologists, disparities in diagnostic ability, and the need for establishing diagnostic methods for cases where early detection is fundamentally difficult using conventional techniques. Medical photonics, an engineering field that applies optical technologies to meet medical needs such as diagnosis and treatment, is a promising next-generation technology capable of solving these problems. Leading examples include Raman spectroscopy[2], near-infrared imaging[3], and fluorescence imaging[4]. These technologies are non-invasive and feature high spatial resolution and real-time performance. However, their implementation in society remains highly limited due to the immaturity of the technologies and the high barriers peculiar to the medical field. ULVAC-The University of Osaka Joint Research Laboratory for Future Technology has begun collaborative efforts with researchers from the School of Medicine and the School of Engineering at the University of Osaka to address these social issues.

1.2 Malignant traits of cancer

When cancer is fatal, the tissue often possesses malignant traits that are expressed through genetic abnormalities during the proliferation process. The malignant traits of cancer are invasiveness, where cancer cells spread while destroying surrounding tissue, and metastasis, where the cells settle and proliferate in other tissues via lymphatic or blood vessels, and the pathological features associated with these traits are highly diverse[5]. Numerous characteristics that confer these properties to malignant cancers have been reported and are broadly classified into molecular characteristics and morphological characteristics. For example, cancer cells must have the ability to detach from the primary site in order to invade other tissues; in other words, the ability to produce molecules that inactivate proteins responsible for cell adhesion[6]. Furthermore, metastasis requires that cancer cells be capable of adhering to the target organ, which is explained by their affinity for selectin molecules that are normally responsible for capturing leukocytes[7]. In this report, we refer to such characteristics acquired through the functions and interactions of biomolecules as “molecular characteristics”. Furthermore, some morphological characteristics have been reported, such as the tissue structure of malignant cancers[8] and differences in

*Related findings were presented at the 85th JSAP Autumn Meeting (Japan Society of Applied Physics).

*1 Research Laboratory for Future Technology, Research & Development HQ, ULVAC, Inc.
(2-1 Yamadaoka, Suita, Osaka 565-0871, Japan)
*2 Graduate School of Engineering, The University of Osaka
(2-1 Yamadaoka, Suita, Osaka 565-0871, Japan)
*3 Graduate School of Medicine, The University of Osaka
(2-1 Yamadaoka, Suita, Osaka 565-0871, Japan)

the density of microvilli on cell surfaces[9]. Although information on malignancy is crucial for treatment strategies and prognostic assessment, it is usually difficult to obtain non-invasively, and treatment is often no longer possible by the time the information has been visualized enough to facilitate identification.

1.3 Polarization analysis of biological tissue

One proposed non-invasive optical method of diagnosing biological tissue involves the use of circularly polarized light (CPL)[10]. Polarized light is light in which the electric field vector oscillates according to specific rules. In particular, CPL is a state in which the oscillation traces a circular path within a plane perpendicular to the direction of light propagation. Light diffusely reflected within biological tissues experiences various optical events such as reflection, refraction, absorption and scattering. This information should be preserved as changes in parameters that define the state of the light, such as wavelength, intensity and polarization state (Fig. 1). In particular, polarization analysis is considered to be useful for non-invasive analysis of complex systems such as biological tissue. This is because the polarization state of light changes when it interacts with molecular or morphological characteristics. For example, many biomolecules that confer molecular characteristics to malignant cancers, such as enzymes, proteins, lipids and amino acids, exhibit chirality, or circular dichroism (meaning interactions differ depending on the rotation direction of CPL). Although studying the chirality of biomolecules within biological tissue and their effects is challenging, it is widely recognized in pharmacology that the pharmacological properties of a substance can vary depending on its chirality[11]. Furthermore, polarization state is altered by light scattering, and the scattering characteristics are greatly influenced by morphological features[12]. Moreover, because the permeability, scattering probability and penetration depth of light in biological tissue will vary depending on the wavelength of light, those characteristics may be associated with spatial information. Therefore, being able to analyze the polarization state changes of white light that has been diffusely reflected within biological tissue and its wavelength dependence is expected to enable both the malignancy and spatially localized distribution of cancers to be estimated. For reasons such as this, medical photonics that uses polarized light is considered to be a promising next-generation diagnostic technology. However, the samples, measurement methods and analysis techniques of previous studies are entirely different[10),13], and the resulting phenomena inadequately interpreted. It can therefore be said that medical applications of technology that use polarized light have yet to be established. Moreover, previous studies have been limited to discerning cancerous tissues from normal tissues, which alone is likely insufficient to replace existing technologies. This study therefore aims to develop polarization-based medical photonics technology capable of obtaining advanced pathological information via practical methods. Here, “advanced pathological information” refers to the structural and cytological characteristics of biological tissues, as well as their correlation with disease properties, which cannot be obtained through conventional pathological diagnostic methods. In this study, we first investigated measurement and analysis methods by using the broadband visible CPL transmission method on human lungs.

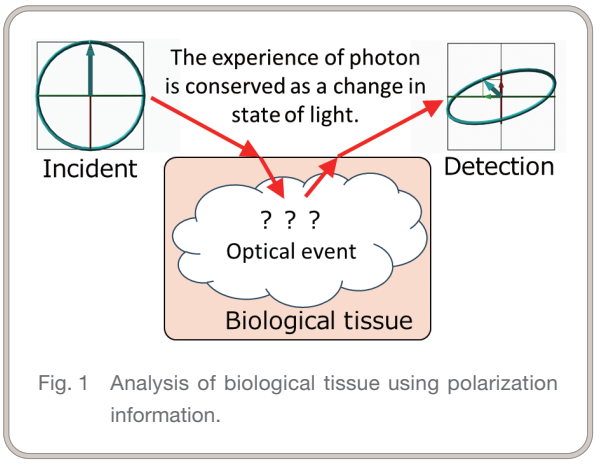

Fig. 1 Analysis of biological tissue using polarization information.

2. Visible circular polarization characteristics of human lung adenocarcinoma

2.1 Experimentation techniques

2.1.1 Samples

BEAS-2B normal cells and A549 cancer cells derived from human lungs were both cultured in glass petri dishes. Additionally, two human lung adenocarcinoma specimens, one non-metastatic and one metastatic, were fixed, embedded and sliced into 4 μm thin pieces. Hematoxylin-Eosin (HE) staining was also performed, with the samples being sealed between a glass slide and cover glass. Fig. 2 shows the appearance of each sliced sample (a: non-metastatic, b: metastatic). In either

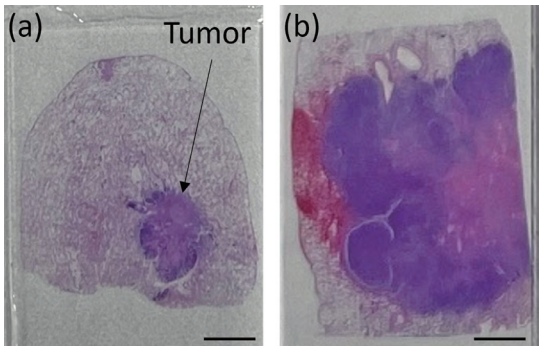

Fig. 2 Appearance of the sliced (4 μm) tissue samples of (a) non-metastatic and (b) metastatic human lung adenocarcinoma stained with hematoxylin and eosin (scale bar: 5 mm). The dense (dark purple) and sparse regions are tumor and normal tissues, respectively.

case, the densely packed regions correspond to tumors, while the surrounding sparse regions show normal tissue. Also, Fig. 3 shows an optical microscope image of the non-metastatic sample (a: tumor, b: normal). The purple-stained grains are cell nuclei, of which the relatively large and dark-colored ones are cancer cell nuclei and the small and light-colored ones are normal cell nuclei, and the red grains of about 5 μm are red blood cells.

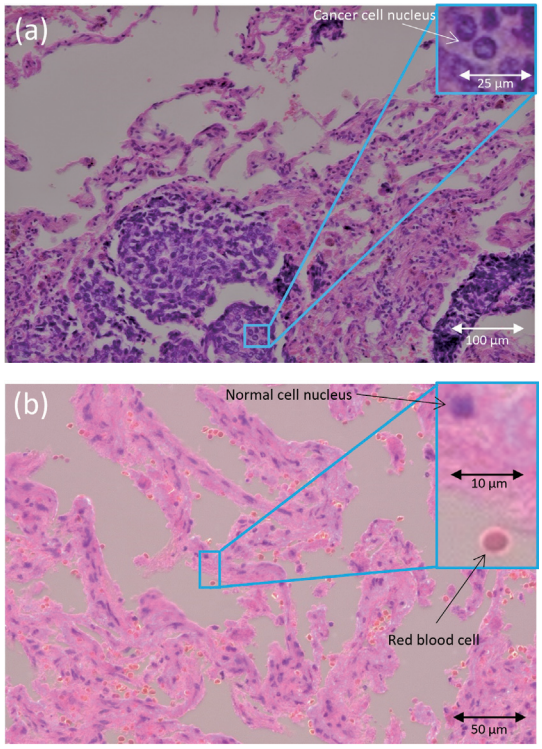

Fig. 3 Optical microscope images of (a) tumor and (b) normal regions of a sliced (4 μm) tissue sample of non-metastatic human lung adenocarcinoma stained with hematoxylin and eosin. The purple-stained grains are cell nuclei, where the relatively small and pale ones are normal cell nuclei, and the large and dark ones are cancer cell nuclei. The red grains of approximately 5 μm are red blood cells.

2.1.2 Measurement and analysis methods

Left-handed circularly polarized light (LCP) or right-handed circularly polarized light (RCP) was applied vertically to both the cultured cells and sliced samples, and the circular polarization degree (CP) of the transmitted light was measured using the polarizer rotation method. When measuring the sliced samples, tumor and normal regions were identified based on their stained appearance, and CPL was directed into each region for measurement. Fig. 4 shows a schematic diagram of the optical system, while Fig. 5 shows the spectrum of the incident light source. In this configuration, a linear polarizer (LP) was rotated 360 degrees, and light intensity was measured at 15-degree intervals. Then, the profile of the light intensity was fit to a sinusoidal function with respect to the LP rotation angle and used to calculate the CP at each wavelength. Here, CP is defined as

$$CP = |I_L - I_R| / (I_L + I_R) \quad \text{(Formula 1)}.$$

I_L and I_R represent the light intensities of LCP and RCP, respectively. Also, the depolarization ratio (DR) is defined as

$$DR = (CP_{BKG} - CP_{sample}) / CP_{BKG} \quad \text{(Formula 2)}.$$

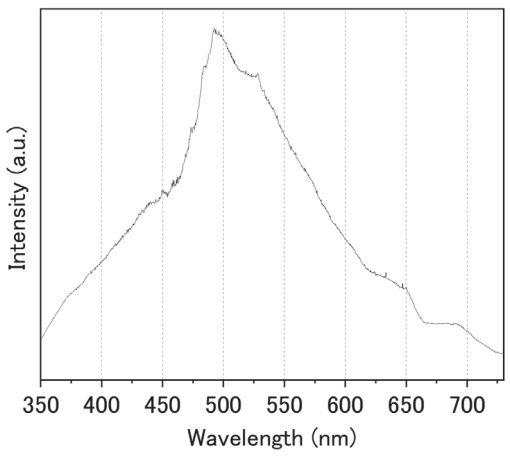

Fig. 5 Incident light spectrum.

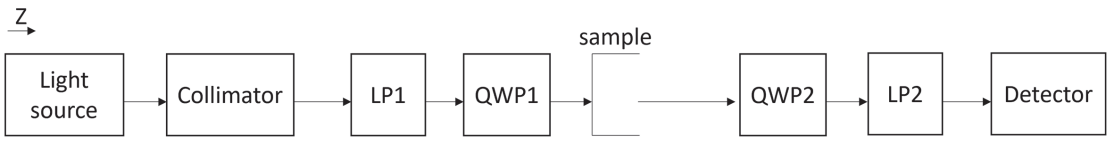

Fig. 4 Schematic diagram of circularly polarized light transmission measurement system for samples. The light from the source was collimated and circularly polarized by passing it through a collimator, a linear polarizer (LP) and a quarter wave plate (QWP). The circularly polarized light was incident vertically (Z axis) from the bottom of the samples. The circular polarization degree of the transmitted light was measured by the polarizer rotation method.

CP_{BKG} and CP_{sample} refer to the CP of light transmitted through only the sample holder (glass petri dish + culture medium or cover glass + slide glass) and the CP of light transmitted through biological samples, respectively. Using the DR makes it possible to evaluate changes in the CP derived from biological samples. Furthermore, the circular dichroism (CD) of the DR is defined as

$$CD = DR_L - DR_R \quad \text{(Formula 3)}.$$

DR_L and DR_R are the DR when the incident light is LCP and RCP, respectively. These polarization parameters were compared to evaluate the visible circular polarization characteristics of each sample.

2.2 Results and discussion

Fig. 6 shows the DR wavelength dependence of cultured cell samples. It was observed that the depolarization ratio of cancer cells A549 is greater than that of normal cells BEAS-2B, becoming more significant at longer wavelengths. This is inferred to be due to differences in the size of the scatterers (primarily cell nuclei) in the sample[12]. In general, the size and pleomorphism of cell nuclei are greater in cancer cells than in normal cells, with the same trend being observed in the cultured cell samples used

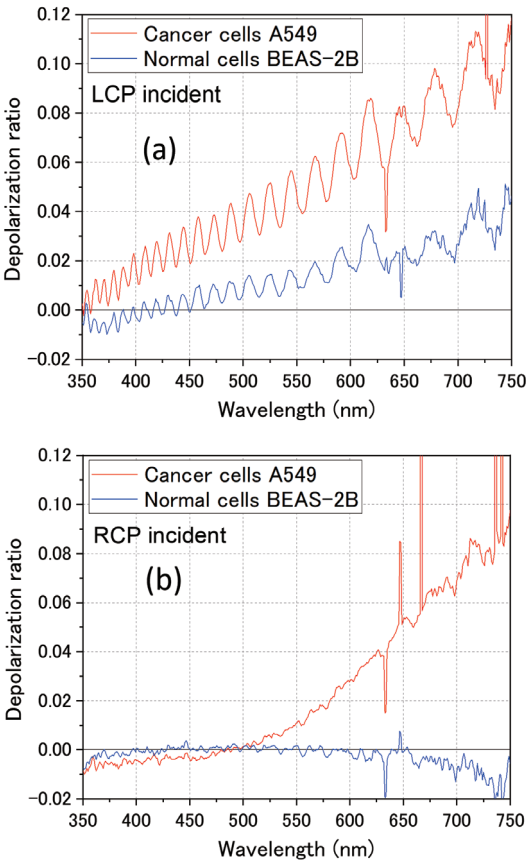

Fig. 6 Wavelength dependence in depolarization ratio of normal and cancerous cultured cells measured with (a) LCP and (b) RCP incidence.

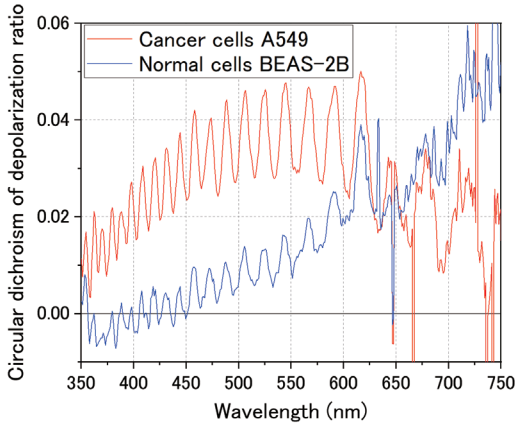

Fig. 7 Wavelength dependence in circular dichroism of depolarization ratio of normal and cancerous cultured cells.

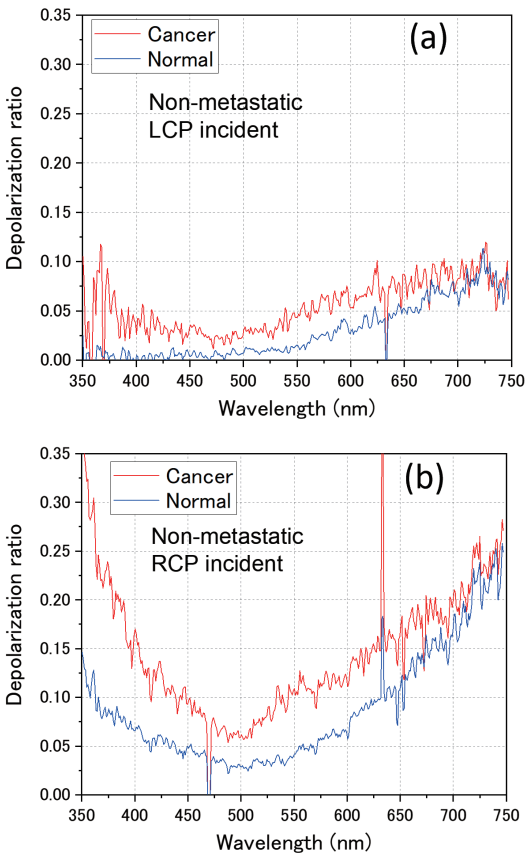

Fig. 8 Wavelength dependence in depolarization ratio of non-metastatic sliced tissue sample measured with (a) LCP and (b) RCP incidence.

in this experiment. Also, cancer cells exhibit higher CD values in the wavelength range of 350–650 nm (Fig. 7). Although this may be attributed to differences in the distribution of chirality among biomolecules, further investigation is required.

Fig. 8 and Fig. 9 show the DR wavelength dependence of non-metastatic and metastatic sliced samples, respectively. In the measured wavelength range, the DR was found to be larger in the tumor regions. The same trend can also be observed for CD in Fig. 10. These polarization parameters therefore suggest the potential for discerning tumor regions from normal regions. However, at first glance, there appears to be no clear difference in the trends based on the presence or absence of metastasis in these results. Although it is difficult to quantify the different CD levels in tumor and normal regions, the metastatic samples tended to show a greater difference (Fig. 11).

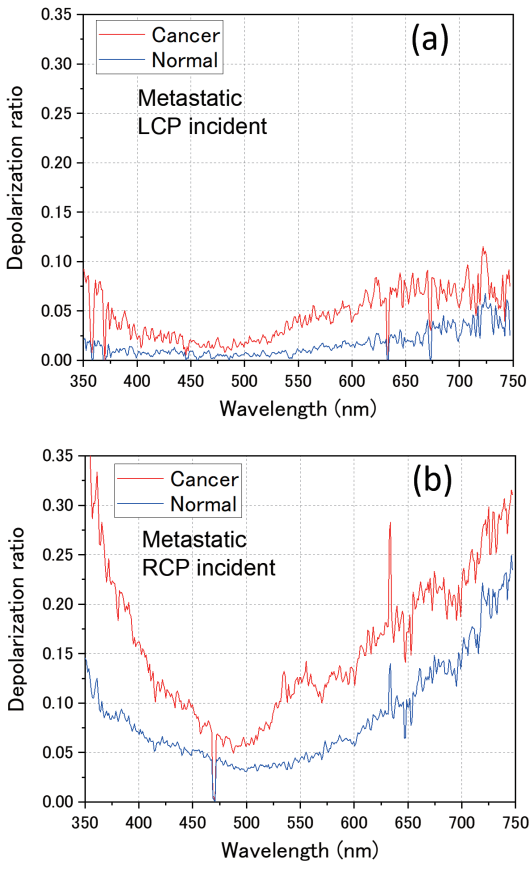

Fig. 9 Wavelength dependence in depolarization ratio of metastatic sliced tissue sample measured with (a) LCP and (b) RCP incidence.

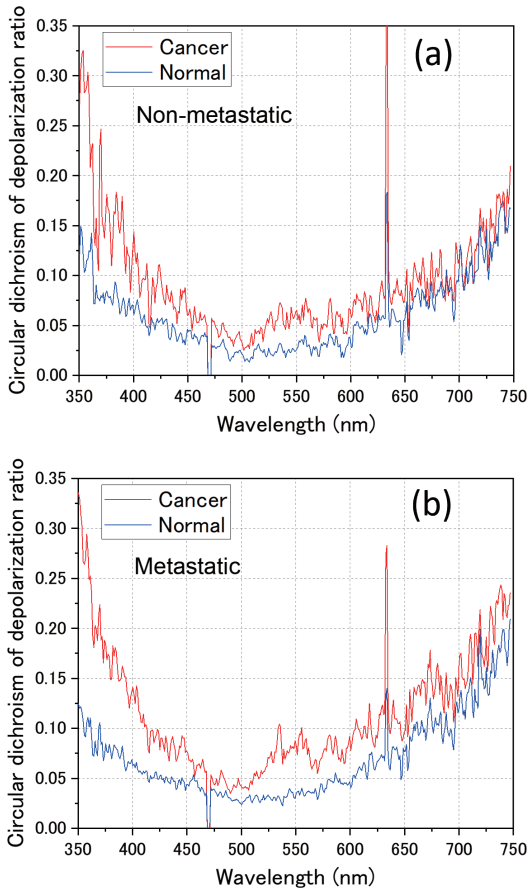

Fig. 10 Wavelength dependence in circular dichroism of depolarization ratio of (a) non-metastatic and (b) metastatic sliced tissue samples.

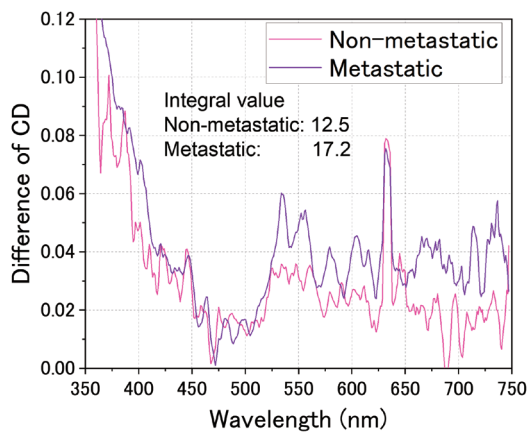

Fig. 11 Wavelength dependence in the difference of circular dichroism of depolarization ratio between tumor and normal regions of non-metastatic and metastatic sliced tissue samples.

3. Summary and future outlook

The results of our study focused on the broadband visible circular polarization characteristics of human lung adenocarcinoma and suggest the possible application of depolarization ratios (DR) and circular dichroism (CD) parameters in discerning cancer cells from normal cells and evaluating cancer malignancy. However, the elementary processes of changes in polarization parameters are still not well understood, and sufficient cases have not been verified to date. Therefore, in this study, we will continue to evaluate and analyze the circular polarization characteristics of specimens of known cases, and systematize the correlation between the circular polarization characteristics of biological tissue and advanced pathological information. However, in the measurements performed using the transmission method in this study, the proportion of detected light subjected to optical events originating from the biological sample is considered to be very small, posing a challenge when it comes to improving the reliability of quantitative evaluations on polarization parameter changes. Furthermore, the transmission method is impractical for clinical situations such as endoscopic applications. Therefore, the diffuse reflection method is considered to be effective, and validation has already begun. As an additional effort, we will attempt to clarify the mechanisms of polarization parameter changes by constructing a physical model capable of explaining the circular polarization characteristics of biological samples, using phantom experiments and electromagnetic field simulations. Finally, we will aim to propose an algorithm for estimating advanced pathology information from optimal measurement conditions (e.g., wavelength, polarization, light intensity, detection angle), analysis parameters and analysis results.

Incidentally, the investigation of circular polarization characteristics in human cancers is a novel endeavor from both engineering and medical perspectives. Although the application potential of CPL is not limited to medical photonics and includes high-density information communication[14], novel principle-based storage media[15] and 3D displays[16], its social implementation does remain limited. Despite the asserted potential for CPL to radically solve fundamental societal challenges inherent in the fields of information communication and computing, its technological development has yet to show signs of progressing beyond the realm of academic research, which may be attributed to two key factors. One is the absence of practical CPL microdevices. Although not touched upon in this manuscript, we are also engaged in research on such devices. Secondly, engineering that treats the scalar degrees of freedom of light (wavelength and intensity) as information has already become a part of social infrastructure in modern society, and because so many systems depend on this approach, there is a lack of immediate applications for engineering that treats the degrees of freedom of polarization states as information. Having few applications—or in other words, no demand from society—means that device development will not advance, and without practical devices, application technologies will also fail to progress. Therefore, we recognize the need to develop CPL application technology capable of being combined with existing technologies to meet urgent social needs. This research is one effort towards achieving that goal. In closing, we hope that these studies serve as a catalyst for bringing about a future society in which high value-added photons can play an active role in all areas.

References

1) Ministry of Health, Labour and Welfare: “Annual Report of Monthly Vital Statistics (2020)”.
2) K. Mizushima, Y. Kumamoto, S. Tamura, M. Yamanaka, K. Mochizuki, M. Li, S. Egoshi, K. Dodo, Y. Harada, N. I. Smith, M. Sodeoka, H. Tanaka, K. Fujita: Sci. Adv., **10**, eadn0110 (2024).
3) T. Takamatsu, R. Fukushima, K. Sato, M. Umezawa, H. Yokota, K. Soga, A. Hernandez-Guedes, G. M. Callico, H. Takemura: Opt. Express., **32**, 16090 (2024).
4) Z. Long, J. Gan, X. Wang, X. Jiang, Y. Zou, S. Huang, X. Zhang, Y. Wei: Eur. Polym. J., **222**, 113608 (2025).
5) S. Hirohashi: Proceedings of the 119th Japanese Association of Medical Sciences Symposium, p. 6 (2001).
6) H. Akedo, M. Mukai: Kagaku to Seibutsu (Chemistry and Biology), **36**, 565 (1998).
7) M. Kitano, Y. Kizuka, T. Sobajima, M. Nakano, K. Nakajima, R. Misaki, S. Itoyama, Y. Harada, A. Harada, E. Miyoshi, N. Taniguchi: J. Biol. Chem., **296**, 100354 (2021).
8) N. M. Novikov, S. Y. Zolotaryova, A. M. Gautreau, E. V. Denisov*: Br. J. Cancer*, **124**, 102 (2021).
9) J. Hamada, J. Ren, and M. Hosokawa: Electron-microscopy, **31**, 81 (1996).
10) N. Nishizawa, B. Al-Qadi, T. Kuchimaru: *J. Biophotonics*, **14**, e202000380 (2021).
11) Y. Hamashima, K. Yamashita: Chem. Educ., **70**, 258 (2022).
12) B. Kunnen, C. Macdonald, A. Doronin, S. Jacques, M. Eccles, I. Meglinski: *J. Biophotonics*, **8**, 317 (2015).
13) D. Ivanov, V. Dremin, E. Borisova, A. Bykov, T. Novikova, I. Meglinski, R. Ossikovski: Biomed. Opt. Express, **12**, 4560 (2021).
14) J. F. Sherson, H. Krauter, R. K. Olsson, B. Julsgaard, K. Hammerer, I. Cirac, E. S. Polzik, Nature, **443**, 557 (2006).
15) C. D. Stanciu, F. Hansteen, A. V. Kimel, A. Kirilyuk, A. Tsukamoto, A. Itoh, Th. Rasing: Phys. Rev. Lett., **99**, 047601 (2007).
16) M. Ahmad, J. Li, H. Ma, J. Liu: Displays, **85**, 102848 (2024).